NURETH14-214

TRANSIENT VOID, PRESSURE DROP AND CRITICAL POWER BFBT BENCHMARK ANALYSIS AND RESULTS WITH VIPRE-W / MEFISTO-T

J. M. Le Corre, C. Adamsson¹ and P. Alvarez

Westinghouse Electric Sweden AB 72163 Västerås, Sweden

lecorrjm@westinghouse.com, carl.adamsson@psi.ch, alvarep@westinghouse.com

Abstract

A benchmark analysis of the transient BFBT data [1], measured in an 8x8 fuel assembly design under typical BWR transient conditions, was performed using the VIPRE-W/MEFISTO-T code package. This is a continuation of the BFBT steady-state benchmark activities documented in [2] and [3]. All available transient void and pressure drop experimental data were considered and the measurements were compared with the predictions of the VIPRE-W sub-channel analysis code using various modeling approaches, including the EPRI drift flux void correlation. Detailed analyses of the code results were performed and it was demonstrated that the VIPRE-W transient predictions are generally reliable over the tested conditions. Available transient dryout data were also considered and the measurements were compared with the predictions of the VIPRE-W/MEFISTO-T film flow calculations. The code calculates the transient multi-film flowrate distributions in the BFBT bundle, including the effect of spacer grids on drop deposition enhancement, and the dryout criterion corresponds to the total liquid film disappearance. After calibration of the grid enhancement effect with a very small subset of the steady-state critical power database, the code could predict the time and location of transient dryout with very good accuracy.

Introduction

In the design and safety analysis of Boiling Water Reactors (BWR), it is necessary to accurately evaluate some detailed thermal-hydraulic characteristics of the nuclear fuel assemblies loaded into the core, under both steady-state and transient conditions. For example, the amount of steam produced within the coolant directly impacts the neutron moderation and hence the reactivity feedback and the rod power; the coolant friction along the rods and the local pressure losses impact the reactor pump power requirements and the total coolant flowrate; finally, the redistribution of mass and enthalpy within the rod bundle may impact the reactor thermal margin and hence the allowable maximum core power.

One of the computer codes currently in use for such type of calculations at Westinghouse is the VIPRE-W sub-channel analysis code, which can resolve the transient, one-dimensional mass, momentum and energy distributions in every sub-channel. VIPRE-W is Westinghouse's version of the VIPRE-01 code [4] developed under the sponsorship of the Electric Power Research Institute (EPRI). The VIPRE-W code is currently used for various core thermal-hydraulics risk and safety analysis calculations, in particular for PWR non-LOCA core thermal-hydraulics safety

_

¹ Currently: Paul Scherrer Institute, 5232 Villigen, Switzerland

analysis [5]. The VIPRE-W code can also be coupled with the MEFISTO and the MEFISTO-T film flow analysis tools effectively extending it to a three-field code in the annular flow region and adding the capability of mechanistic liquid film dryout prediction under both steady-state (see e.g. [6]) and transient [7] conditions, respectively.

The critical power in a fuel assembly under typical BWR operating conditions corresponds to the bundle power at which the heat transfer degrades rapidly due to the dryout of the liquid film in annular two-phase flow. This is an important parameter to control and calculate in order to accurately estimate the fuel thermal performance and the margin to the fuel licensing criteria. In core BWR safety analysis, the critical power is calculated using a dryout correlation developed based on a large steady-state, bundle-design specific, dryout database (and also verified against transient dryout experiments). However, a mechanistic approach to this issue is also desirable in order to support the development of new fuel assembly designs and to assess the validity of the dryout correlations under non-tested conditions (e.g. power distributions, various transients, etc). Eventually, it can be expected that a mechanistic approach can replace the correlation approach, provided that the calculations can be performed with reasonable speed and accuracy.

In this paper, the performance of the VIPRE-W/MEFISTO-T code package is assessed against detailed experimental void, pressure drop and dryout transient data measured at the NUPEC/BFBT facility [1]. This work is part of the OECD/NRC BWR Full-Size Fine-Mesh Bundle Test (BFBT) benchmark and is a continuation of the steady-state benchmark analysis performed with the VIPRE-W / MEFISTO code package and documented in [2] and [3].

1. Transient BFBT database and benchmark

The BFBT database is documented in detail in [1]. The experiments were performed by the Nuclear Power Engineering Corporation (NUPEC) at the BWR Full-size Fine-mesh Bundle test (BFBT) facility in Japan. Details concerning the test loop are also available in [1] and will not be repeated here.

The test fuel assembly design used for the transient measurements is of the so-called "high burn-up" fuel assembly type consisting of an 8x8 fuel rod array with one large water rod in the center. The test assemblies have a heated length of 3.708 m and 7 spacer grids with a so-called "ferrule" spacer design, further details can be found in Figure 1. Test assembly 4 (void transient) has uniform axial and non-uniform radial (A) power distributions while test assemblies C2A and C3 (transient dryout) have non-uniform axial (cosine and inlet peaked, respectively) and radial (A) power distributions. The relative radial power distribution (A) is shown in Figure 2; it is observed that the peripheral rods have higher power and hence should yield higher quality/void and hence be more limiting in terms of dryout.

1.1 BFBT transient void database

Two typical BWR transients were simulated in the BFBT experiments with void measurements: Turbine trip without bypass and Recirculation pump trip. Initial conditions were selected near nominal BWR operating conditions (Exit pressure = 7.16 MPa, Power = 4.5 MW, Flowrate = 55 t/h and inlet temperature = 279 °C). The power, flowrate, inlet/outlet pressure and inlet temperature transient boundary conditions are shown on Figure 3 and Figure 4.

Item	Data				
Test assembly					
	4	C2A	C2B	C3	
Simulated fuel assembly type		High b	ourn-up 8×8		
Number of heated rods			60		
Heated rods outer diameter (mm)	12.3				
Heated rods pitch (mm)	16.2				
Axial heated length (mm)	3708				
Number of water rods	1				
Water rods outer diameter (mm)	34.0				
Channel box inner width (mm)	132.5				
Channel box corner radius (mm)	1 8.0 1				
In channel flow area (mm²)			9463		
Spacer type]	Ferrule		
Number of spacers			7		
Spacer pressure loss coefficients			1.2		
Spacer location (mm)	455, 967, 1479, 1991, 2503, 3015, 3527 (distance from bottom of heated length to spacer bottom face)				
Radial power shape	A	A	В	A	
Axial power shape	Uniform	Cosine	Cosine	Inlet-peak	

[○] Heated rod,

Water rod – no flow in water rods

Figure 1 "High burnup" assembly geometry and power distribution [1]

1.15	1.30	1.15	1.30	1.30	1.15	1.30	1.15
1.30	0.45	0.89	0.89	0.89	0.45	1.15	1.30
1.15	0.89	0.89	0.89	0.89	0.89	0.45	1.15
1.30	0.89	0.89			0.89	0.89	1.15
1.30	0.89	0.89			0.89	0.89	1.15
1.15	0.45	0.89	0.89	0.89	0.89	0.45	1.15
1.30	1.15	0.45	0.89	0.89	0.45	1.15	1.30
1.15	1.30	1.15	1.15	1.15	1.15	1.30	1.15

Figure 2 Radial power distribution "A" used for transient tests [1]

During the transient, chordal-averaged void fractions were measured at elevations 0.682, 1.706 and 2.730 m using X-ray densitometers and 5 cm downstream the end of heated length, using the X-ray CT scanner. However, the BFBT transient void database reports only the assembly cross-section averaged void fraction [1]. A densitometer correction factor provided to the BFBT benchmark participants (see details in e.g. [8]) was also applied to the experimental measurements (for void fraction higher than 0.2, [8]).

A: Simulation pattern for beginning of operation.

B: Simulation pattern for middle of operation.

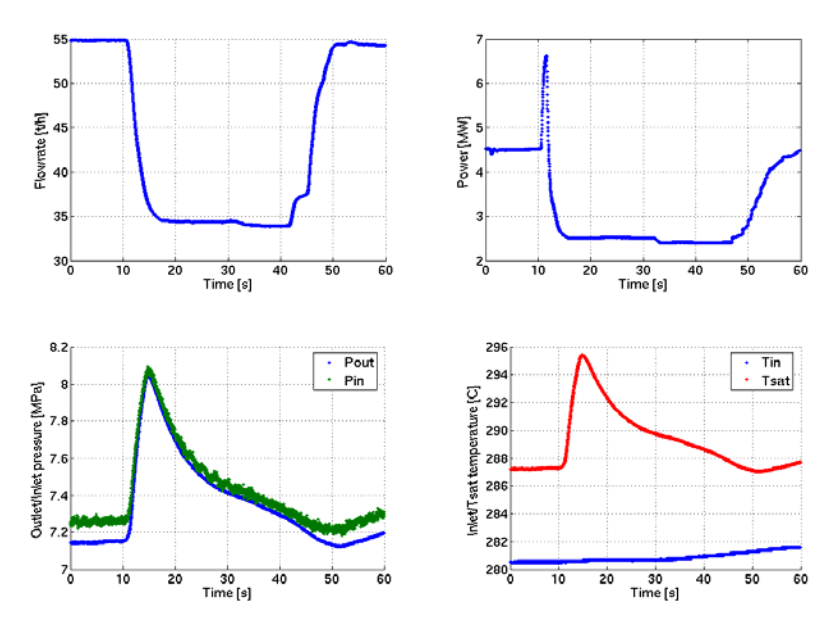


Figure 3 Turbine trip without bypass transient boundary conditions for the void experiments

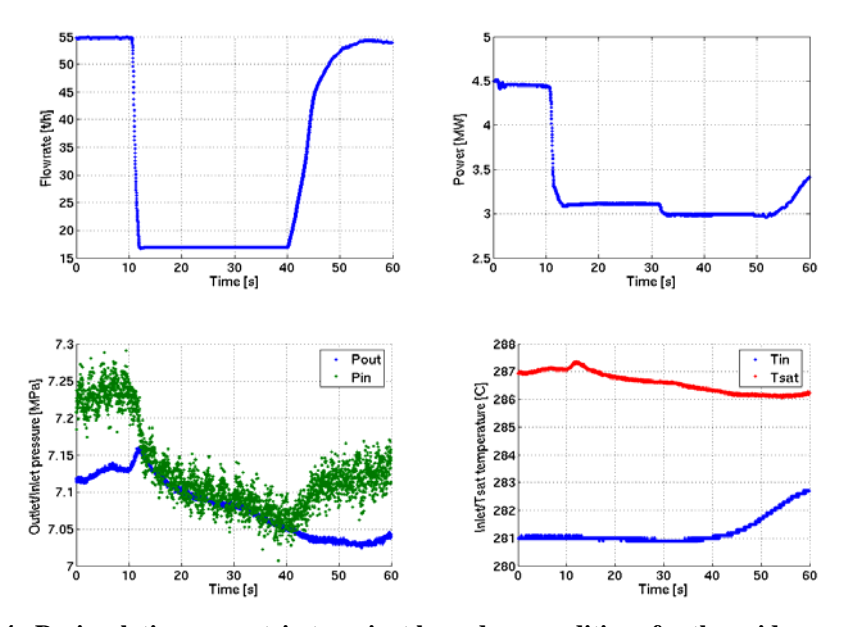
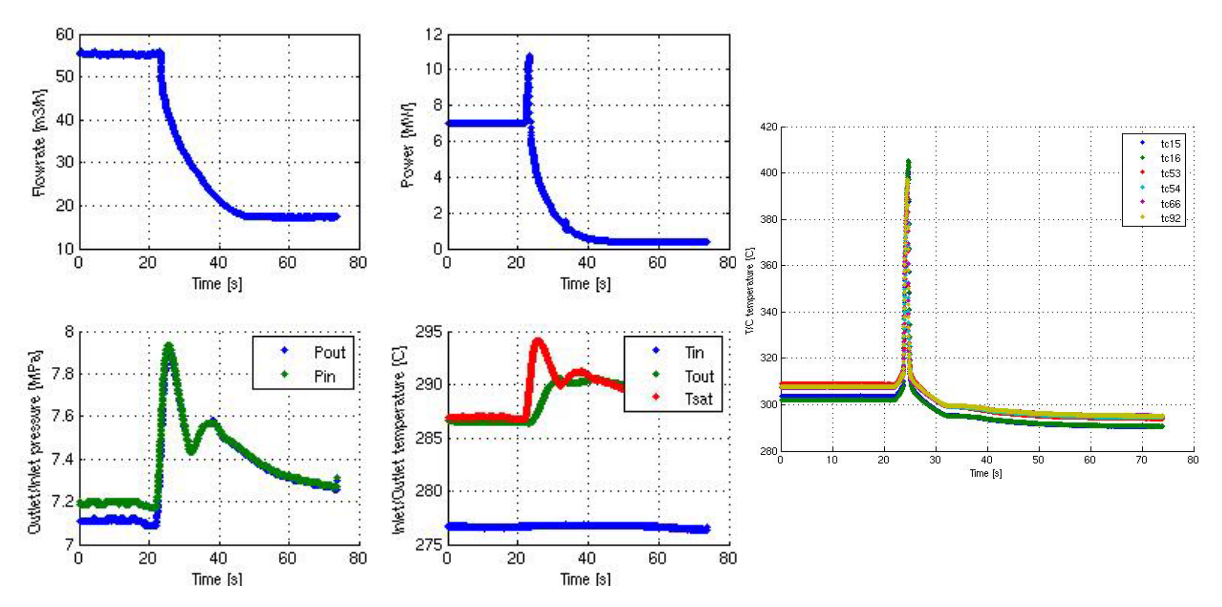


Figure 4 Recirculation pump trip transient boundary conditions for the void experiments

1.2 BFBT transient critical power database

The same typical BWR transients as in the void experiments were simulated in the transient critical power measurements. Initial conditions were also similar except for the bundle power that was set higher so that about 15% margin to critical power remains at the initiation of the transient (See Section 5.1). The power, flowrate, inlet/outlet pressure and temperature boundary conditions are shown on Figure 5 and Figure 6. The BFBT specifications [1] limit the analysis to the Cosine power tests only. However, all tests (Cosine and Inlet peaked power) were considered herein in order to study the effect of the axial power distribution on the dryout location.

The radial and axial geometry of the test section is illustrated in Figure 7, along with the thermocouple (T/C) locations used for the dryout detection (shown for assembly C2A only). It can be noted that the thermocouples are placed in locations where dryout is the most expected, i.e. on the highest powered boundary rods, just upstream the three uppermost grids. The measured T/C traces are shown on Figure 5 and Figure 6.



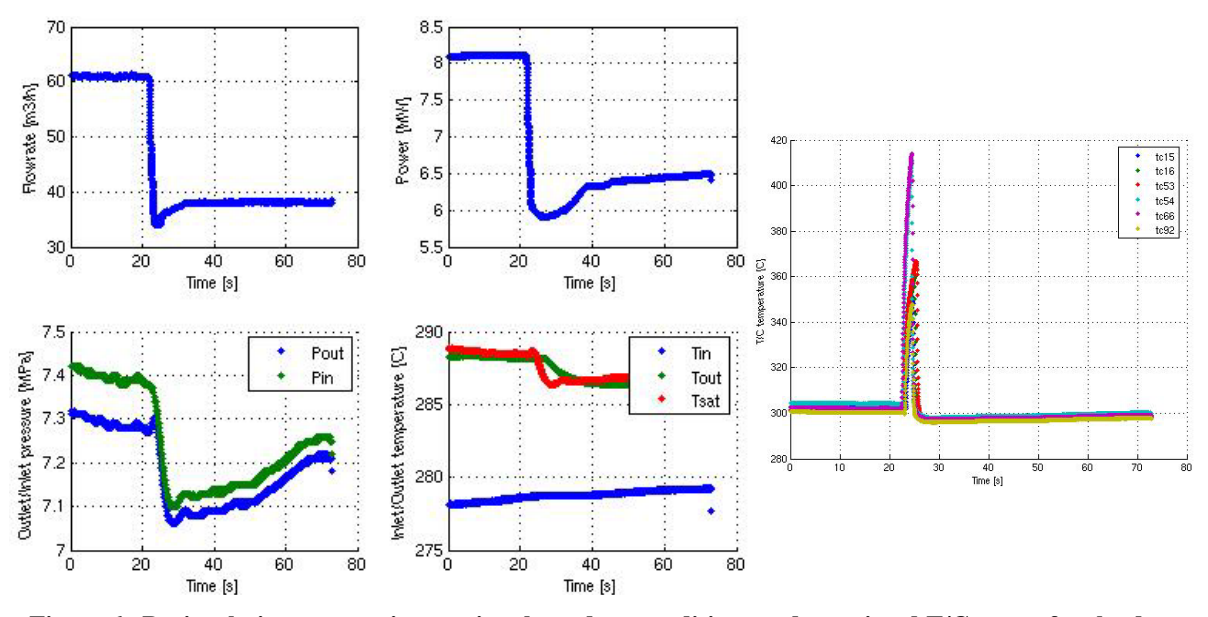


Figure 6 Recirculation pump trip transient boundary conditions and associated T/C traces for the dryout experiments

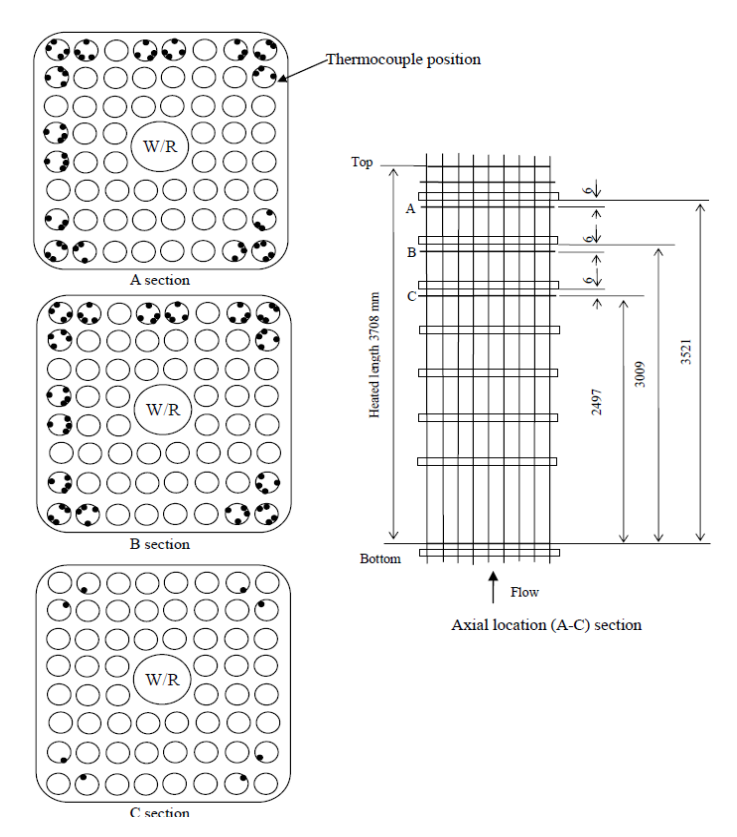


Figure 7 BFBT bundle radial and axial geometry and thermocouple locations for Assembly C2A [1]

1.3 BFBT transient pressure drop database

The BFBT transient pressure drop database is extracted from both the transient void and the transient dryout experiments where both the assembly inlet and outlet measured pressure were reported. Hence, six transient tests are available for the comparison with the code predictions.

2. VIPRE-W / MEFISTO-T code package

2.1 VIPRE-W sub-channel analysis code

VIPRE-W is Westinghouse's version of the VIPRE-01 MOD-02 code [4] which contains additional features and enhancements for reactor core design applications [5]. However, within the scope of this work, no difference between VIPRE-01 MOD-02 and VIPRE-W is expected.

The available VIPRE-01 models are described in detail in [4]. The code resolves the mass, momentum and enthalpy conservation equations for the two-phase mixture (three-equation model) and the void is calculated via a constitutive relation. Alternatively, the mass conservation equation for the vapor phase can also be solved along with a drift flux velocity accounted for in the mixture momentum equation (four-equation drift flux model). The list of selected VIPRE-01 closure models relevant to BWR applications (except for the heat transfer model which is not relevant to steady-state) is documented in [2] and is kept unchanged in this transient analysis:

- Blasius type friction coefficient fitted to the single-phase pressure drop experiments + EPRI two-phase friction multiplier
- Constant local loss coefficients, fitted to the single-phase pressure drop experiments + Romie two-phase local loss multiplier
- EPRI subcooled boiling model
- EPRI bulk (drift flux) void model. Alternatively, the four-equation drift flux two-phase flow model was also tested
- Diversion and turbulent mixing, see [2]
- Dittus-Boelter correlation for convective & Thom correlation for subcooled and saturated nucleate boiling heat transfer (post-dryout heat transfer is not modeled, see Section 2.2)
- EPRI and Bowring CHF correlations for dryout (independent from MEFISTO-T predictions)
- 100 axial nodes

2.2 MEFISTO-T transient film flow analysis code

MEFISTO-T is a transient film flow analysis code developed by Westinghouse which is intended to work as a post-processor to any transient two-phase sub-channel analysis driver code, effectively extending it to a three-field code and adding the capability of mechanistic dryout prediction [7]. The steady-state version of the code has been extensively validated (see [3], [6]). The approach results in a highly robust and computationally efficient transient three-field solution within the bundle (Section 6). VIPRE-W (Section 2.1) was selected as the transient sub-channel driver code due to its known robustness, fast execution speed, and potential for accurate calculation under typical BWR operating conditions. The overall VIPRE-W/MEFISTO-T calculation chain is shown on Figure 8. A summary of code models and past validations is documented in this Section.

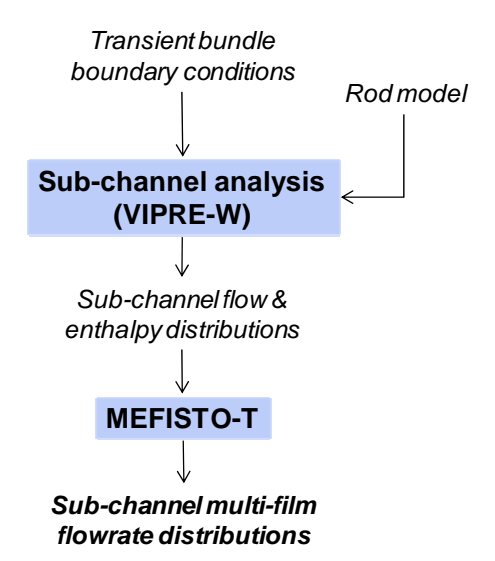


Figure 8 VIPRE-W/MEFISTO-T calculation chain

A practical approach was taken where mass and energy balance couplings with neighboring subchannels are pre-calculated by a dedicated transient sub-channel analysis code and the transient film flow equations are simplified to be applicable to annular two-phase flow considering length and time scales prevailing in BWR fuel assemblies. These simplifications were first considered and tested by comparison with a complete three-field approach solution and transient dryout tests in pipe [9]. These simplifications were further theoretically and numerically verified in [7]. Further details regarding the MEFISTO-T modeling approach, including the treatment of partlength rods, drop deposition enhancement due to spacer grids, can be found in [6] and [7].

The same entrainment and deposition correlations as in the steady-state validations ([3] and [6]) were used in this work. In addition, the drop deposition enhancement factor used in this work was inherited from the steady-state BFBT benchmark analysis [3] without any modification. Hence, the MEFISTO-T code does not require any additional empirical parameter as compared to the steady-state analysis.

This approach results in a fast and robust transient multi-film solution in the BWR bundle. In the case of the BFBT bundle, each time step were calculated with a runtime = 7.8 CPU seconds using a standard 3 GHz Intel Xeon processor.

2.3 Steady-state performance

The VIPRE-W/MEFISTO code package has been extensively validated under steady-state conditions, using the BFBT steady-state void, pressure drop and critical power database [3] and using the FRIGG Optima3 critical power database [6]. In the case of the steady-state BFBT benchmark, the entire steady-state cross-section averaged exit void database, restricted to outlet pressure > 1.4 MPa (351 data points), was predicted with an absolute mean error (M-P) of -0.016 and a standard deviation of 0.021 [2]. After calibration of the grid enhancement effect with a very small subset of the critical power database, the MEFISTO code could extrapolate to the remaining database with a mean error of 1.5% and a standard deviation of 3.5% [3].

Hence, the performance of the code is comparable to fuel bundle design-specific CPR correlations for the prediction of critical power and has also superior dryout location prediction capability. Note that a code performance assessment to the level performed in steady-state is not possible for transient applications due to the lower availability and more complex interpretation of test data (in particular, the experimental margin to dryout). However, the aim is to look for sufficient justifications that the code performances are maintained from steady-state applications to transient analysis.

3. BFBT transient void analysis and results

3.1 Preliminary analysis of void test data

The provided transient void data at the transient initiation were compared to similar void measurements from the BFBT steady-state database to check for consistency. The comparison is presented in Table 1.

It can be observed that the void measurements (without correction) and the VIPRE-W predictions are consistent for the densitometer measurements. However, the CT scanner void measurements at the transient initiations seem too low (as compared to both similar steady-state measurements and VIPRE-W predictions) and therefore are deemed unreliable for this benchmark exercise.

•				•	
	Stead	y-state	Transient (initial)		
Test	4101-59	4101-60	4102-01	4102-19	
Pressure [MPa]	7.19	7.18	7.14	7.11	
Power [MW]	4.88	4.89	4.53	4.50	
Flowrate [t/h]	54.57	54.62	54.83	54.76	
Inlet subcooling [kJ/kg]	52.1	50.5	35.9	31.7	
Target x _{out} [-]	0.18	0.18	0.18	0.18	
BFBT/VIPRE CT void	0.737/0.740	0.740/0.742	0.681 /0.737	0.699 /0.739	
BFBT/VIPRE DEN1 void	0.735/0.660	0.733/0.663	0.739/0.664	0.747/0.668	
BFBT/VIPRE DEN2 void	0.567/0.503	0.568/0.508	0.583/0.528	0.588/0.537	
BEBT/VIPRE DEN3 void	0 174/0 174	0 173/0 181	0 197/0 239	0 234/0 266	

Table 1 Steady-state vs. transient initiation void measurements and predictions

3.2 Comparison with predictions

The transient void measurements at the four considered elevations (Section 1.1) during the two provided transients are compared with the VIPRE-W predictions in Figure 9.

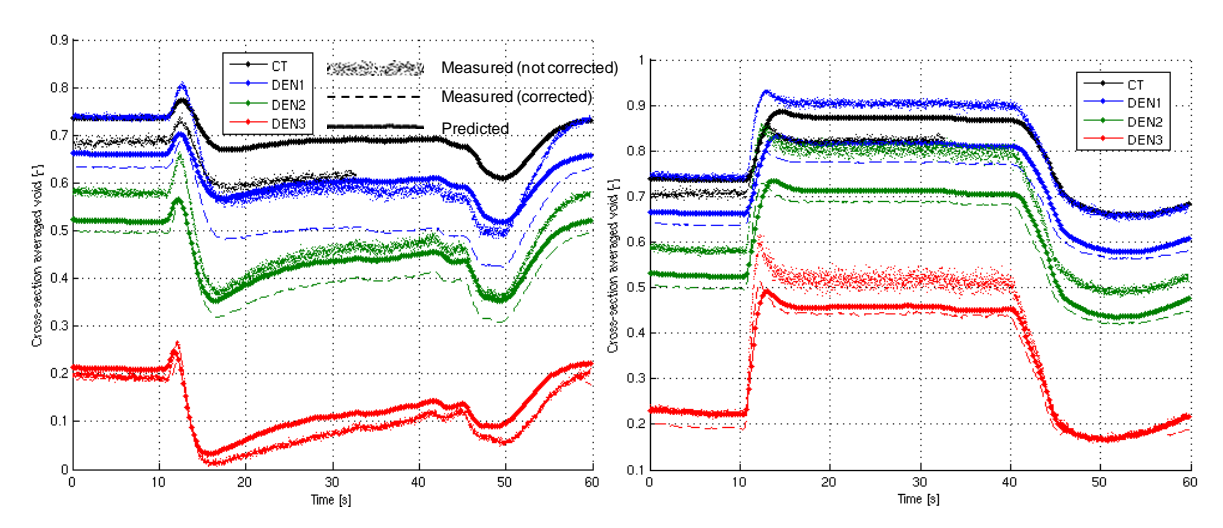


Figure 9 BFBT/VIPRE-W comparison for Turbine trip without bypass test (left) and Recirculation pump trip (right)

The differences observed in Table 1 can be seen at the transient initiation. These differences remain stable during the transient with slight improvement/deterioration. However overall, the performance of the steady-state code predictions is maintained during the transient. As expected (Section 3.1) the VIPRE-W void predictions are away from the measurements at the CT location.

Various VIPRE-W settings were modified and compared. The change from single-channel to sub-channel analysis, from local pressure to exit pressure consideration and from high (100

nodes) to low (25 nodes) axial resolution had an effect only on the cross-section averaged void measured in the lower part of the bundle (DEN3) where the bulk flow is still subcooled. This is due to local non-equilibrium effects which are affected by the bundle design (hot vs. cold subchannels) and the saturation line position. However the observed differences were well below the code prediction uncertainties and are hence assessed to be negligible.

The four-equation drift flux model (section 2.1) was also used and compared to the measured void. However, and similar to the observation documented in [2] in steady-state, the code prediction performance deteriorates as compared to the results calculated using a three-equation model and the EPRI drift flux void correlation. Hence the four-equation model was not considered further.

4. Transient pressure drop analysis and results

4.1 Preliminary analysis of pressure drop data

The provided transient assembly pressure drop data (from beginning to end of heated length) at the transient initiation were compared to similar pressure drop measurements from the BFBT steady-state database to check for consistency. The comparison is presented in Table 2.

	Steady-state		Transient (initial) Void tests		
Test	P60009	P60010	4102-01	4102-19	
Pressure [MPa]	7.17	7.17	7.14	7.11	
Power [MW]	4.20	5.31	4.53	4.50	
Flowrate [t/h]	55.0	54.9	54.83	54.76	
Inlet subcooling [kJ/kg]	51.1	47.3	35.9	31.7	
Target x _{out} [-]	0.15	0.20	0.18	0.18	
BFBT/VIPRE DP [kPa]	78.6/72.8	93.2/83.0	106.4 /79.7	101.5 /80.3	

Table 2 Steady-state vs. transient initiation pressure drop measurements and predictions

It can be observed that VIPRE-W slightly underpredicts the pressure drop measurements in steady-state. However, the measured pressure drop at the transient initiation become significantly higher while VIPRE-W predicts a value in-between the steady-state measurements (consistently with the target x_{out}). Note that different inconsistencies were also observed during steady-state stages of the transient (when the measured pressure remain constant), e.g. for the Recirculation pump trip the pressure drop was measured higher than the steady-state pressure drop under similar conditions. Hence, this needs to be considered in the comparison with the code predictions since the experimental transient data might not be reliable.

4.2 Comparison with predictions

The transient pressure drop measurements during the two provided transients are compared with the VIPRE-W predictions in Figure 10.

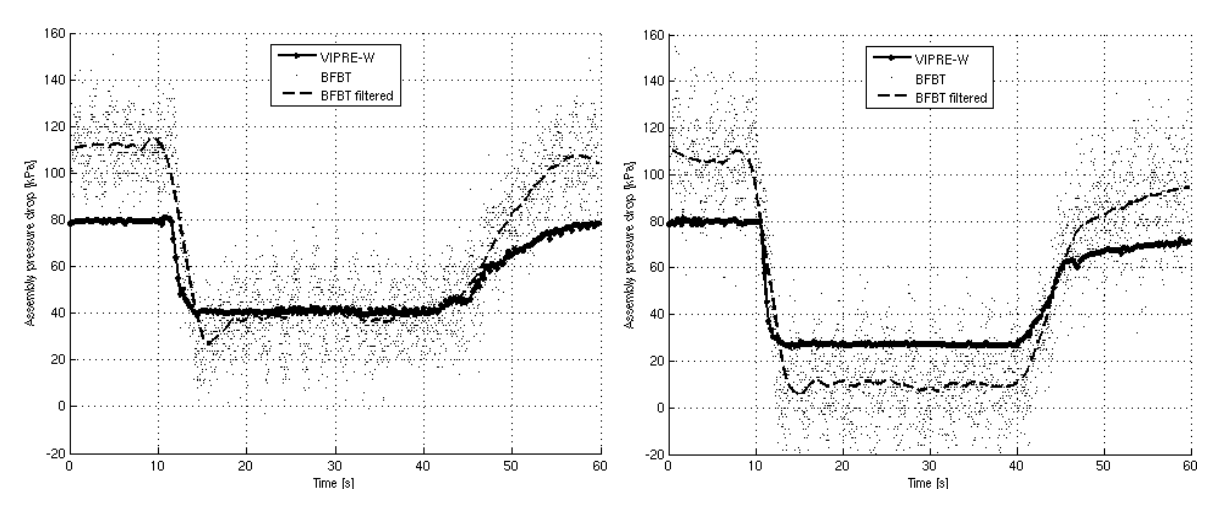


Figure 10 BFBT/VIPRE-W comparison for Turbine trip without bypass test (left) and Recirculation pump trip (right)

The large differences observed in Table 2 are shown at the transient initiation. This difference decreases at lower flow and even reverses in the case the Recirculation pump trip test. However, the transient pressure drop measurements were assessed to be inconsistent with the steady-state data (Section 4.1) at the transient initiation (higher measurement) but also during steady-state stages of the transients (lower measurement in the case of the recirculation pump trip). Hence, only the relative change in pressure drop can be compared with relevant meaning. The four additional assembly pressure drop measurements from the transient dryout database were also tested and the results and trends were identical. In general, the relative change in pressure drop is well predicted by the code.

Table 3	Steady-state vs.	. transient initiation	power measurements

	Steady (Critical		Transient (Initial conditions)			
Test	SA616500 (C2A)	SC616500 (C3)	TGA10008 (C2A)	TRA10012 (C2A)	TGC10018 (C3)	TIC10012 (C3)
Pressure [MPa]	7.13	7.15	7.11	7.31	7.10	7.26
Power [MW]	8.30	8.61	7.04	8.09	7.18	7.18
Flowrate [t/h] [m³/h]	45.17	45.04	41.93 55.40	46.18 61.13	41.91 55.13	46.22 61.11
Inlet subcooling [kJ/kg]	54.21	50.88	54.1	57.0	59.8	58.2
MEFISTO predicted Critical Power [MW]	8.18	8.61				
Initial margin to DO [%]			15.2	2.5	16.6	16.6

5. Transient dryout analysis and results

5.1 Preliminary analysis of dryout data

The imposed initial powers of the dryout transient tests were compared with steady-state critical power at the same conditions from the BFBT steady-state database. The available margin to dryout at each transient initiation was estimated using the corresponding measured critical power from the steady-state experiments under similar conditions. The results are presented in .

The comparison shows that the dryout transient tests were initialized at about 15 to 16% below the critical power except for test TRA10012 which was initialized with only 2.5% margin to critical power (with a 1.5% uncertainty on the measured power [1]) which is considered questionable. We will assume in the following analysis that there is no error in the provided database, however experimental data from test TRA10012 might not be reliable.

5.2 Comparison with predictions

The transient T/C traces measurements during the two provided transients are compared with the VIPRE-W/MEFISTO-T predicted minimum film flowrate and VIPRE-W CPR calculations in Figure 11 for the Turbine trip without bypass and Figure 12 for the Recirculation pump trip.

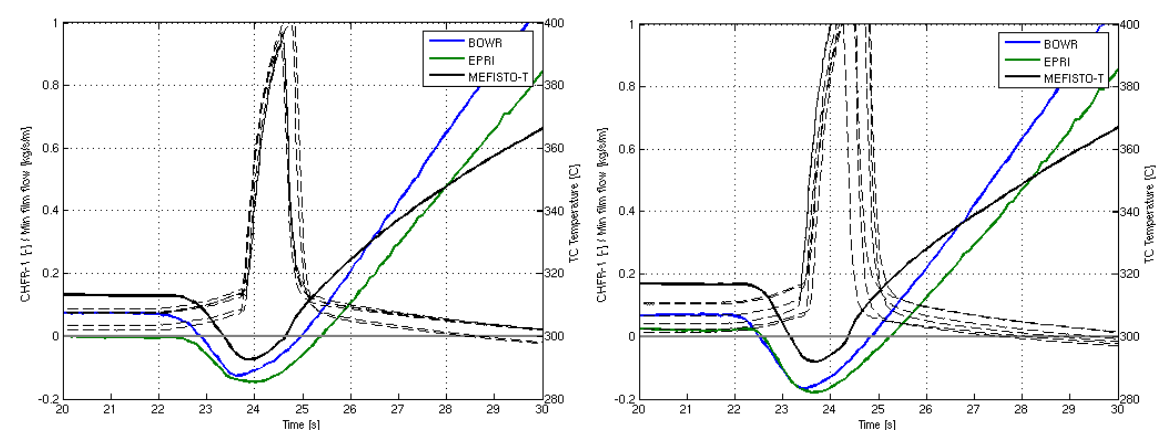


Figure 11 BFBT T/C traces and VIPRE-W/MEFISTO-T min film flowrate and CHFR-1 for Turbine trip without bypass test, Cosine power (TGA, left) and Inlet peaked power (TGC, right)

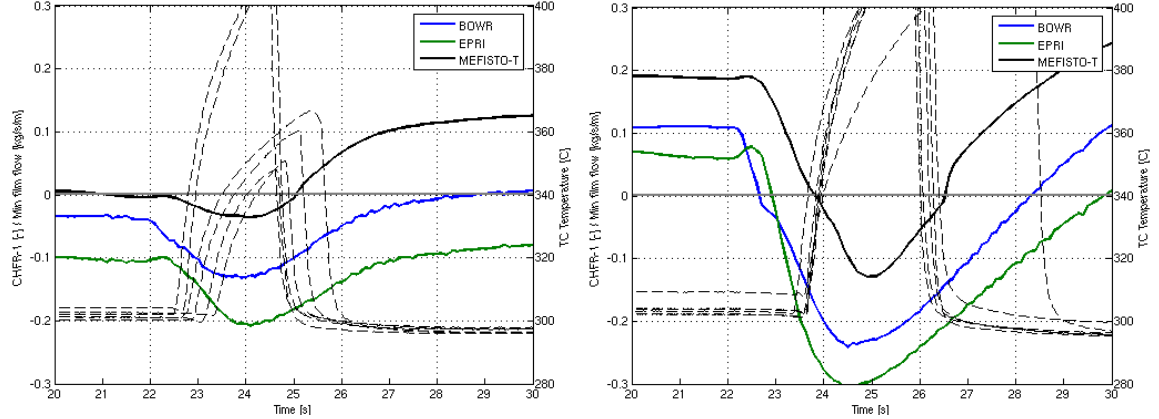


Figure 12 BFBT T/C traces and VIPRE-W/MEFISTO-T min film flowrate and CHFR-1 for Recirculation pump trip test, Cosine power (TRA, left) and Inlet peaked power (TIC, right)

It can be observed that the MEFISTO-T dryout predictions are in general delayed as compared to the CPR correlation predictions and in better agreement with the T/C measurements. In the case of Test TRA10012 (Figure 12, left), the CPR correlations predict the transient in dryout from initiation, while MEFISTO-T yields a very small margin. The observation for this particular test is not unexpected and stems from the observations discussed in Section 5.1.

The VIPRE-W/MEFISTO-T film flowrate and CPR distributions in the most limiting subchannels at the predicted time of dryout (by MEFISTO-T) are provided in Figure 13 for the Turbine trip without bypass and Figure 14 for the Recirculation pump trip. The film flowrate distributions are plotted for all surrounding walls (i.e. four distributions) but yield very similar values for equal rod power (hence only two different distributions are visible in this subchannel). The T/C locations are indicated by letters (A to D immediately downstream the four upper grids) and are shown in red when indicating dryout (i.e. a burst in temperature is experimentally observed).

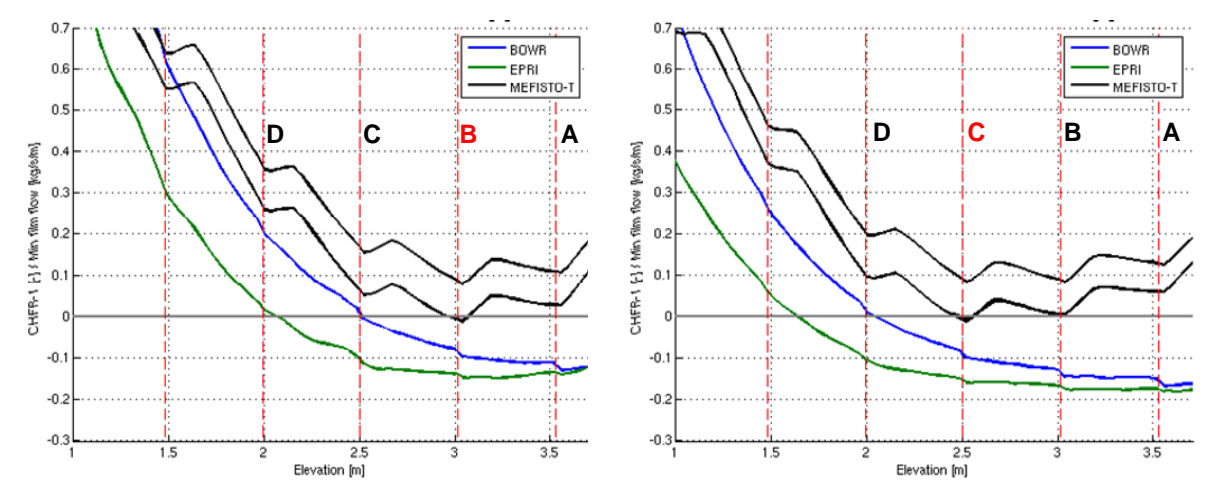


Figure 13 VIPRE-W/MEFISTO-T axial film flowrate and CHFR-1 distributions for Turbine trip without bypass test, Cosine power (TGA, left) and Inlet peaked power (TGC, right). T/C measured in dryout are red

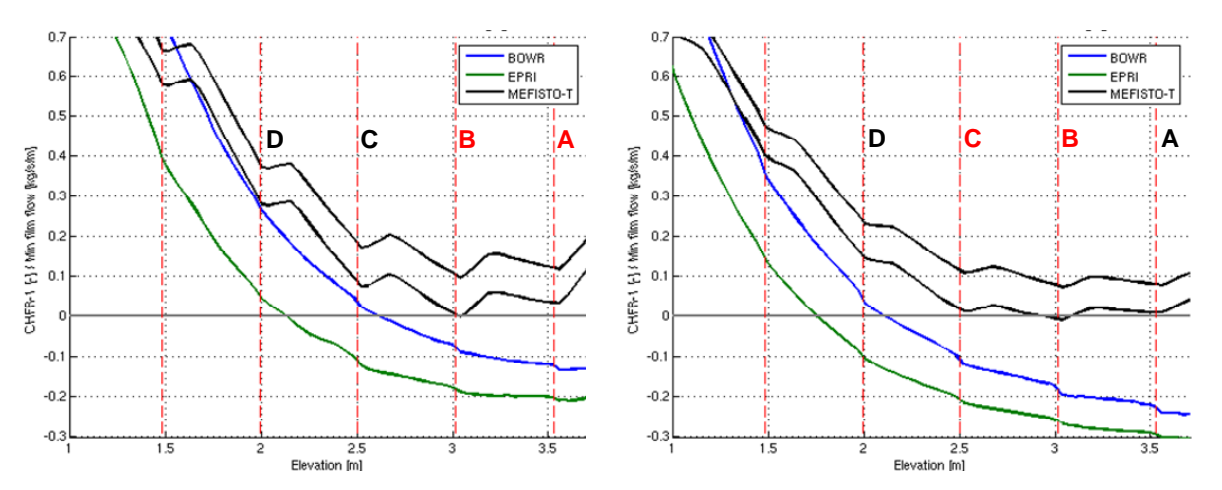


Figure 14 VIPRE-W/MEFISTO-T axial film flowrate and CHFR-1 distributions for Recirculation pump trip test, Cosine power (TRA, left) and Inlet peaked power (TIC, right). T/C measured in dryout are red

The non-monotonic nature of the film flow solution from MEFISTO-T, due to the drop deposition enhancement downstream the grids, can be clearly observed on the Figures. The MEFISTO-T code predicts the correct T/C in dryout, including the shift toward upstream T/C for the Inlet peaked power tests (TGC, TIC) as compared to the Cosine power tests (TGA, TRA). On the contrary, the CPR correlation predicts the occurrence of dryout near the bundle outlet in all cases.

The MEFISTO-T multi-film flow distributions in all considered sub-channels, all surrounding walls, at the most limiting time during the transient, are presented in Figure 15 for the Recirculation pump trip test with Cosine power (TGA10008). The sub-channels predicted in dryout are plotted with red background while the other sub-channels are plotted with blue background. The locations of detected dryout (based on T/C data) are represented by yellow circles. Note also that the BFBT experimental database reports a maximum of six T/C only for all tests and it cannot be excluded that other T/C also experience dryout.

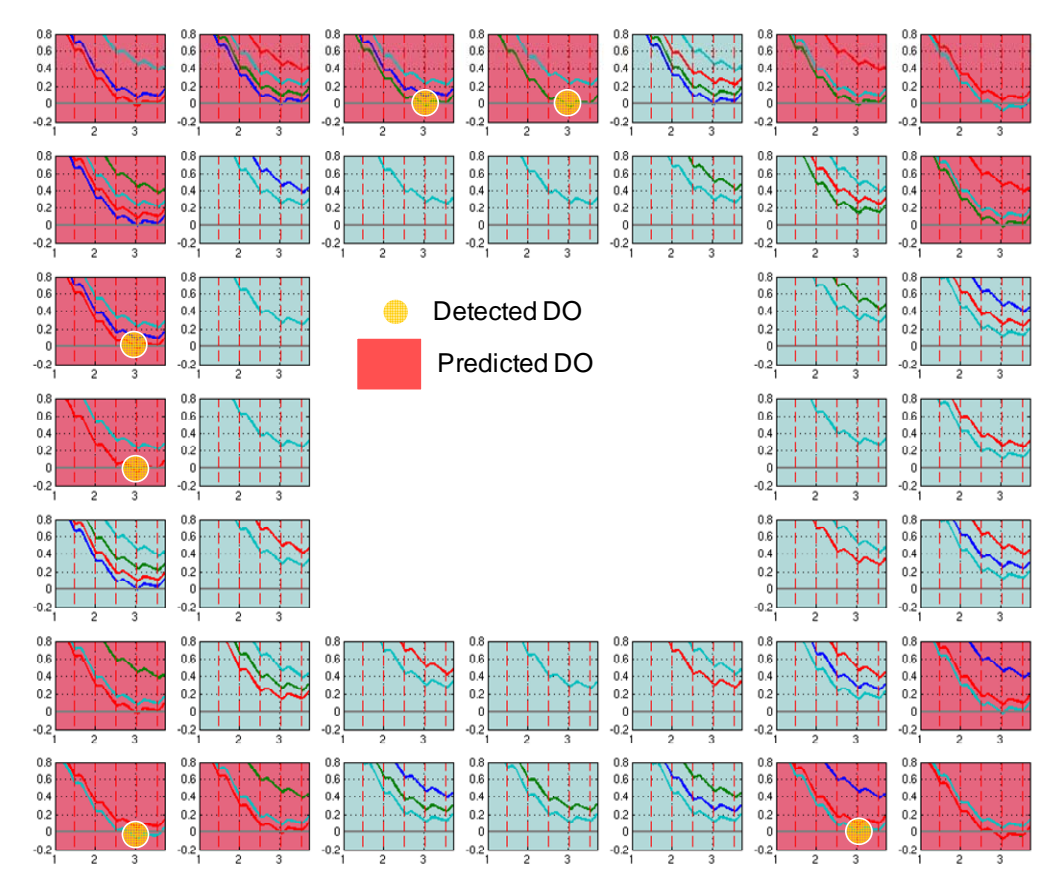


Figure 15 MEFISTO-T axial film flowrate distributions in all considered sub-channels for Recirculation pump trip test, Cosine power (TGA). T/C locations measured in dryout are represented by yellow circles

It can be observed that both the axial and radial locations of the MEFISTO-T predicted dryout are in excellent agreement with the experiments. This agreement was also observed for the other transient dryout tests, with the exception of test TRA10012, however the reliability of this test might be questionable (Section 5.1).

The film flowrate distributions from Figure 15 are color-mapped (in term of film thickness) to the BFBT bundle geometry in Figure 16, considering the whole bundle (left), half of the bundle (center) and three hot channels (right). This provides a realistic overview of the MEFISTO-T code prediction capabilities where four film distributions are calculated for each rod. The dryout locations can be clearly seen (in red) and it can be qualitatively observed that the differences in film flow within the same sub-channel are larger than the differences within the same rod, showing the adequacy of the sub-channel, four-film, approach.

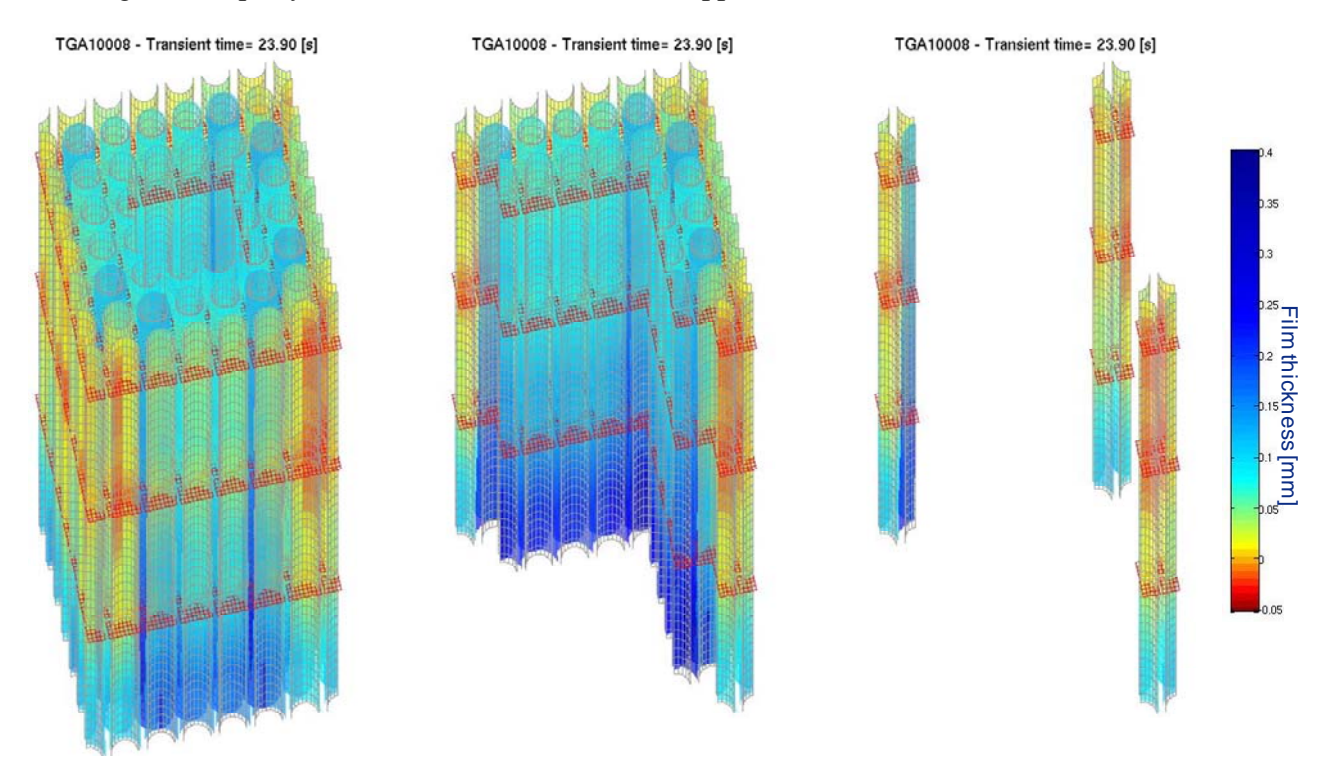


Figure 16 MEFISTO-T film thickness 3D distributions for Recirculation pump trip test (at time=23.90 s), Cosine power (TGA), from 2 meter elevation to the outlet

6. Conclusion

In this work, the performance of the VIPRE-W/MEFISTO-T sub-channel analysis code package was assessed against the available NUPEC/BFBT transient sub-channel void (2 transients), pressure drop (6 transients) and dryout (4 transients) experiments under BWR operating conditions. The database allows the investigation of transient variations in boundary conditions such as the system pressure, the inlet flowrate, the inlet subcooling as well as the axial power distribution. A summary of the selected VIPRE-W models and the MEFISTO-T film flow methodology (for mechanistic liquid film dryout prediction) was presented along with the code-to-data benchmark analysis. The results show that the VIPRE-W code generally has reasonable prediction capability with regard to transient void prediction, consistently with its steady-state performance. In addition, the results show that the VIPRE-W/MEFISTO-T code package has excellent mechanistically-based prediction capability with regard to transient dryout, including time of occurrence, axial dryout elevation and radial dryout location.

7. References

- [1] B. Neykov, F. Aydogan, L. Hochreiter, K. Ivanov, H. Utsuno, F. Kasahara, E. Sartori and M. Martin, OECD-NEA/US-NRC/NUPEC BWR Full-size Fine-mesh Bundle Test (BFBT) Benchmark, Volume I: Specifications, OECD 2006, NEA No. 6212, NEA/NSC/DOC(2005)5.
- [2] K. Brynjell-Rahkola, J.-M. Le Corre and C. Adamsson, "Validation of VIPRE-W subchannel void predictions using NUPEC/BFBT measurements," 13th International Topical Meeting on Nuclear Reactor Thermal Hydraulics (NURETH-13), Kanazawa, Japan, Sept. 27 Oct. 2, 2009.
- [3] C. Adamsson and J.-M. Le Corre, "Validation of film flow analysis code MEFISTO with NUPEC/BFBT dryout measurements," 13th International Topical Meeting on Nuclear Reactor Thermal Hydraulics (NURETH-13), Kanazawa, Japan, Sept. 27 Oct. 2, 2009.
- [4] C. W. Stewart, J. M. Cuta, A. S. Koontz, J. M. Kelly, K. L. Basehore, T. L. George and D. S. Rowe, VIPRE-01: A thermal-hydraulic code for reactor cores, EPRI-NP-2511-CCM-A-Vol.1-Rev.3 (1989).
- [5] Y. X. Sung, P. Schueren and A. Meliksetian, VIPRE-01 Modeling and Qualification for Pressurized Water Reactor Non-LOCA Thermal-Hydraulic Safety Analysis, WCAP-15306-NP-A, Westinghouse Electric Company LLC (1999).
- [6] C. Adamsson and J. M. Le Corre, "Modeling and validation of a mechanistic tool (MEFISTO) for the prediction of critical power in BWR fuel assemblies," *Nucl. Eng. Des.*, in Press, doi:10.1016/j.nucengdes.2011.01.033
- [7] C. Adamsson and J.-M. Le Corre, "VIPRE-W/MEFISTO-T A mechanistic code for transient prediction of dryout in BWR fuel assemblies," 14th International Topical Meeting on Nuclear Reactor Thermal Hydraulics (NURETH-14), Toronto, Canada, Sept. 25–29, 2011.
- [8] M. Glück, "Validation of the sub-channel code F-COBRA-TF: Part II. Recalculation of void measurements," *Nucl. Eng. Des.*, **238**, 9, pp. 2317-2327 (2008).
- [9] J.-M. Le Corre and C. Adamsson, "Development of a new mechanistic tool for the prediction of the liquid film dryout during a transient," 13th International Topical Meeting on Nuclear Reactor Thermal Hydraulics (NURETH-13), Kanazawa, Japan, Sept. 27 Oct. 2, 2009.